Real-Time Hardware-In-The-Loop Implementation of Protection and Self-Healing of Microgrids

Phani Gadde, *Student Member, IEEE,* Sukumar Brahma, *Fellow, IEEE*, Trupal Patel, *Student Member, IEEE,*

***Abstract*—The design of a reliable protection scheme for microgrids often requires communication between protective devices and microgrid controllers. The authors have developed such a communication assisted scalable protection scheme with a self healing feature to protect a microgrid with 100% Inverter Based Resources (IBRs). The communication assisted scheme must be validated in real time with cyber physical co-simulation for successful demonstration. In this regard, the paper presents a co-simulation platform between a simulated power system model using RTDS and physical protective devices. The primary protection of the scheme is programmed in SEL 421-7 relay and backup protection is programmed in MATLAB on a generic computer acting as a microgrid controller. The IEC 61850 models are used to communicate between SEL-421-7 relay and RTDS, whereas TCP/IP communication connects the microgrid controller to RTDS. The paper's focus is to demonstrate the co-simulation platform with communication links established using both protocols and validate the proposed scheme in real-time on the IEEE 123 node distribution feeder. The paper explains the configuration of the IEC 61850 and TCP/IP communications as the interface requires proper hardware and software setup. The real time performance indicates the Hardware In the Loop (HIL) framework as a competent testing environment for the developed protection scheme for microgrids.**

***Index Terms*—Distributed generation, HIL, IEC 61850, microgrid, protection.**

I. Introduction

The bi-directional power flow and multi-mode operation made the protection of microgrids different from protecting conventional distribution systems. The Bi-directional fault currents and current-limited IBRs have rendered the fuse-recloser based schemes infeasible. Hooshyar and Iravani *et al* [1] describe drawbacks of conventional protection schemes in the presence of Inverter Based Resources (IBRs), using transmission and sub-transmission systems for illustration. Brahma [2] analyzes the conventional protection schemes for an IEEE distribution feeder. These papers show that every conventional scheme suffers from a lack of dependability and selectivity, except differential protection, which works well even for systems with 100% IBRs. However, there can always be parts of system that remain radial, where differential principle will not work, making it topology-dependent. It is also financially infeasible to convert a feeder protected by fuses and reclosers into a feeder with relays and breakers at both ends of every section, as would be needed for differential protection.The published solutions to tackle the problem utilize either single or a combination of conventional schemes like over-current, under-voltage, distance and differential protection in addition to schemes that are designed based on harmonics [3], voltage-transients [4] and traveling waves [5]. A number of these solutions depend partially or heavily on communications used for the adaptive setting of relays [6], learning-based relays [7] or more complicated multiagent [8], multilayered [9] protection schemes. These schemes require communication between relays and external devices such as central processing units or microgrid controllers. Although these schemes illustrate success in protecting microgrids, the solutions are mostly valid for the specific topology tested in the paper or too complicated to implement for different system configurations [10]. A microgrid protection scheme should ideally be suitable for any topology, source type, and connection status, and most importantly, cost-effective. Other drawbacks of the published protection schemes are that they are not tested with extremely high (up to 100%) penetration of IBRs, which is a distinct possibility in the near future [11].

To overcome the drawbacks, the authors have developed a protection scheme that is general, scalable, with a self-healing feature in [12]. The proof of concept for the protection scheme with successful detection and isolation of 420 faults of all types is shown in [12]. However, all the analysis is done on IEEE 123 node feeder simulated on non-real-time PSCAD software with simulated communication network delays modeled as a specific value in protective relays (modeled within PSCAD) and microgrid controller (uses PSCAD-MATLAB interface). This is a drawback which can only be addressed by real-time co-simulation of power and communication network (cyber-physical system) with the protective devices interfaced as Hardware In the Loop (HIL) [13]. This setup is called Control Hardware in the Loop (CHIL) simulation. In this paper, the authors present such a HIL framework to establish the cyber and physical setup required to test the developed protection scheme in real-time. Usually, in the published literature, the HIL implementation involves the usage of a single communication protocol in testing protective devices/schemes in closed-loop [14], [15]. In this paper, the authors created a co-simulation platform that uses IEC 61850 and TCP/IP communications to test, analyze, and design a communication-assisted protection and self-healing scheme for microgrids, thus helping to integrate protective devices using different types of protocols. Hence, the novelty of the paper lies in demonstrating a novel communication assisted protection scheme for microgrids in real time that require different types of communication protocols.

P. H. Gadde, S. Brahma and T. Patel are with Holcombe Department of ECE at Clemson University. (e-mail: pgadde,sbrahma,trupalp@clemson.edu).
This work was supported by the 1) U.S.Department of Energy's Office of Energy Efficiency and Renewable Energy (EERE) under the Solar Energy Technologies Office Award Number DE-EE0008774, subaward 20190382-01-CLE and 2) by Clemson University Electric Power Association (CUEPRA).

II. Proposed Protection Scheme

The developed protection scheme in [12] is based on the fundamental principle that short circuit will drive the fault point voltage to a low value and in such a condition, the fault currents will flow into the fault point. To implement this physics, the proposed protection logic uses under voltage monitored directional comparison principle. The scheme does not depend on the type, number, or location of the sources, or the topology of the microgrid, and is scalable with the size of microgrid. The scalability feature is achieved by visualizing the entire microgrid as a network of several physical zones. A zone is the smallest part of the system that can be isolated by opening its boundary breakers. The 123 node distribution feeder shown in Fig. 1 (a) can be treated as a microgrid network that is divided into seven zones and the zonal view is shown in Fig. 1 (b). In this network, for a fault in zone 3, it can be isolated by opening its boundary breakers B3 and B4. Each zone is protected by a relay (hereafter called a "zonal relay"). The zonal relay is considered as the primary protection of a zone. The protection logic is that when a fault brings the voltage below a threshold, only the faulted zone will have currents going into the zone in all of its boundary breakers. So, communication is needed between boundary breakers and zonal relays for primary protection.

The entire microgrid (with multiple zones) is protected by the backup protection residing in the microgrid controller, which is time coordinated with primary protection. The zonal structure in a microgrid resembles a connected graph, and hence the backup protection logic detects the faulted zone using Admittance Matrix (AM) and Node Incidence (NI) matrices used in in graph theory. The AM matrix is built using the breaker status and stores topology information. Where as the NI matrix stores the current direction information in each breaker. Using the same AM matrices, the reconfiguration program in the microgrid controller helps self-heal the system's healthy part after isolation of the faulted zone by the protection system. Detailed explanation of the primary protection logic, backup protection and reconfiguration programs using the AM and NI matrices can be found in [12]. The implementation of the protection scheme and time coordination is explained in section IV.

III. Hardware in the Loop Framework

This section will explain the HIL setup, its components and data flow in detail. The HIL setup consists of the RTDS simulator rack, SEL-2470 software-defined network (SDN) switch, SEL-2488 GPS Clock, SEL-421 protection relay, SDN controller PC, and a Runtime PC as shown in Fig. 2The SEL-2470 SDN switch manages the network traffic between the connected devices. The SDN, the GPS clock, and the SEL 421 relays are configured on a local area network (LAN) and managed using the SDN controller PC. THE SEL-2488 GPS clock provides the GPS time as a PTP signal to the GTSYNC card and the SDN switch. The GTSYNC card synchronizes the simulator time to the GPS time PTP signal.

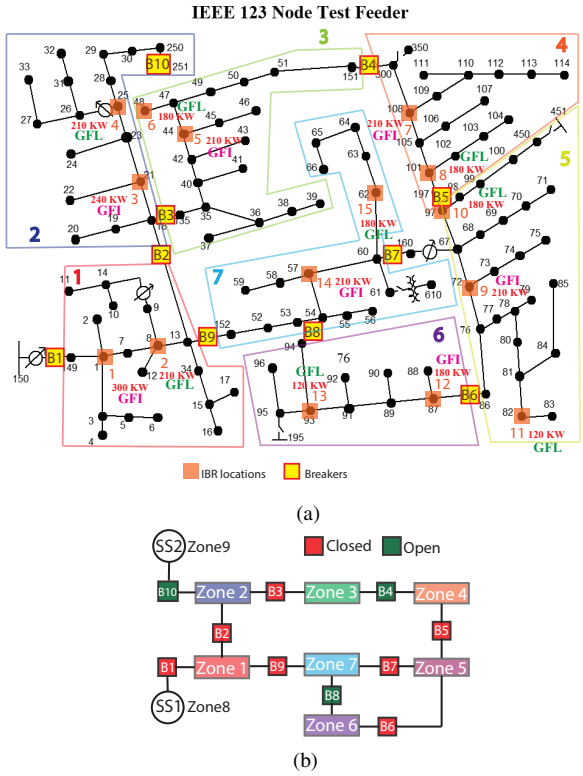

Fig. 1. IEEE 123 node test feeder: (a) one line with IBRs and breaker locations, (b) zonal view diagram with base case breaker status

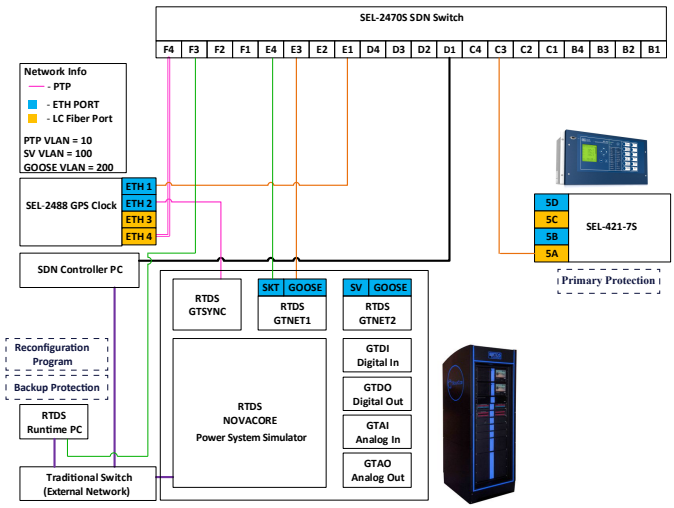

Fig. 2. HIL setup using RTDS.

A. Real-time simulator

The RTDS simulator is designed to perform real-time electromagnetic transient program simulations. The processing unit of the RTDS Simulator is called a NovaCor. Each NovaCor contains an IBM Power8 processor with 10 cores, operating at 3.5 GHz, with workstation interface functionality, communication ports, and analog output channels [16]. These 10 cores are used to solve the network solution, network components (i.e., transmission lines, loads, transformers, etc.,) and any controls present in the simulation modeled using its

user interface software called RSCAD.

1) Microgrid system: The IEEE 123 node test feeder with 15 IBRs is modeled in RSCAD to simulate a microgrid system in real-time. The IBR locations and their ratings are shown in Fig. 1 (a). The inverter models are the building blocks of the 100% IBR based microgrids, and use of detailed models with proper control scheme is vital to enable stable system response for different dynamic scenarios. Authors have developed a detailed switching model of a three-phase inverter based on Proportional Resonant (PR) control in [17]. The performance of this control topology with a robust droop controller is described on the IEEE 13-bus feeder with 4 IBRs, constituting 100% IBR penetration to create the worst-case scenario [18]. However, for the power system side analysis with time frames in the fundamental frequency range (in ms), an averaged model (with full control scheme) can suffice instead of a detailed switching model of the three phase inverter. The switching legs of the IBR models in [18] are averaged as described in [12] to reduce the computational burden and run the microgrid model (123 node power system model + 15 IBR models) in real-time with a time step of $150\mu s$. As seen from Fig. 3, the control of IBRs involves a voltage loop and a current loop operating in separate positive and negative sequence frames. The sequence components are extracted using the Delayed Signal Cancellation (DSC) method [19]. All the inverters operate in grid following (GFL) mode with unity power factor output and supply only balanced currents when the grid is connected, where the grid source supplies reactive power and unbalance currents. This is achieved by employing negative sequence current blocking (NSCB) for calculating the reference for the current control loop after voltage control loop. In islanded mode, one inverter operates in grid forming (GFI) mode. It performs grid functions of keeping voltages balanced while supplying unbalanced currents. This operation is achieved by involving a negative sequence voltage blocking scheme (NSVB) in the voltage control loop. All inverters limit their fault current to a low value for device protection. The value is comparable to their continuous rating (1.1 pu for grid following and 1.5 pu for grid forming were chosen in this study), thus replicating the commercial inverter design [20] in limiting fault currents. The overview of the control diagram of the three-phase IBR model is shown in Fig. 3 and a complete control scheme with a detailed explanation of GFI and GFL mode of operation can be found in [17].

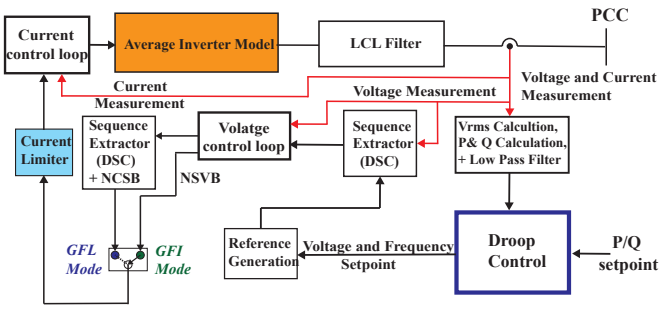

Fig. 3. Overview of three-phase IBR control.

2) IED model: The developed protection scheme requires current directions, breaker status, and voltage magnitude values from all breaker locations shown in Fig. 1 (a). These measurements and breaker controls needed for the protection scheme are modelled in RSCAD as an Intelligent Electronic Device (IED) for each breaker. The breakers are conceived as modern reclosers without using the reclosing function. Modern reclosers are equipped with a control box mounted on the same pole as the recloser, which can be compliant with the communication protocol of choice. The control box can be thought of as an IED that can be programmed to perform different user-defined functions. Since the recloser is equipped with a CT and a VT, and measures voltage and current phasors, different functions related to these phasors can be built into this IED. In the IED, current direction is calculated using the well-established 90-45 directional scheme that uses line voltages as the polarizing quantities for phase units and zero sequence voltage as the polarizing quantity for ground unit [21]. Additionally, these breakers will need to connect two live systems while closing, making it necessary to have a check-synchronization (referred to as "sync-check" hereafter) feature [22] built into the IED. This means after getting a closing signal, the breaker will close only when the voltage and frequency differences between two sides are within allowed thresholds. In addition, the IED is assumed to be able to detect breaker failure (failure to open after a trip command). The manual for a commercially available product [23] shows that these capabilities are already available in modern reclosers, thus validating the assumptions made and the IED model created in RSCAD.

B. Network Interface card for data communication

The GTNETx2 card is used to interface the RTDS to external equipment over a LAN connection using various standard network protocols. The GTNETx2 card can be viewed as a protocol converter accepting packets from the LAN, extracting data from the packets and sending the payload information to the NovaCor processing unit. The GTNETx2 card connects to the NovaCOR via a fiber port. Data from the RTDS Simulation can also be sent into a packet (packet format based on selected protocol) and put out on the LAN where it will be picked up by the devices assigned to accept the data. Each GTNETx2 has the capability of running two protocols simultaneously. In this paper, the GTNETx2 card is configured to use GSE/GOOSE and socket(SKT) protocol [16] for the protection application.

C. SEL-421-7 Relay

The SEL-421-7 relay is a high-speed transmission line protective relay that is compatible with IEC61850 std and features various standard protection logics. SEL provides the acSELerator Quickset software to configure the relay setting either using standard functions or the user can define the custom logic in the place holder called "protection free-form logic settings". As the protection scheme in this paper uses a custom logic developed by the authors, sequence timers, math logic blocks, and latches provided in the acSELerator Quickset software are used to program the protection logic developed

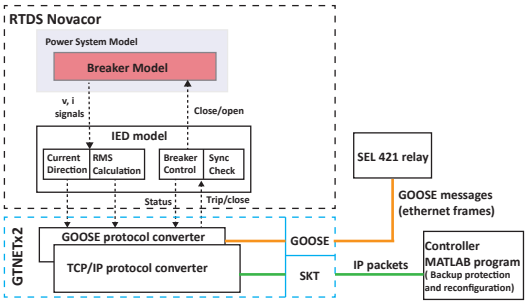

Fig. 4. HIL data flow from RTDS to protection devices.

in [12] as a custom logic. The current direction measurements and breaker status (Boolean value) are received as GOOSE messages by the relay from RTDS. SEL provides relay word bits called virtual bits (VB) for user configuration. The virtual bits $VBXXX$ are used for mapping the receiving GOOSE messages to the relay. Similarly, SEL provides remote analogs (RA) in analog quantities for user configuration. These remote analogs $RAXXX$ are used for mapping RMS voltages from RTDS. The trip signals of the protection logic are mapped onto protection variables $PSVXX$. The protection variables are part of the Boolean variables provided in the SEL relay. These trip signals are configured to be sent as GOOSE messages to RTDS that will be explained in the below section.

D. IEC 61850 Framework

The IEC 61850 standard was developed by the IEC Technical Committee Number 57 Working Group 10 and IEEE for Ethernet (IEEE 802.3)-based communication in electrical substations and is currently being extended for teleprotection (IEC 61850-90-1). Although developed initially, keeping the substation automation and protection in mind, IEC 61850 also works well for microgrid applications. It provides an efficient and reliable interoperability framework between different field devices in protection applications. The protection applications impose stringent restrictions on messages that communicate fault-related signals, such as the 4 ms end-to-end time limitation imposed on GOOSE messages by IEC 61850 [24], making it a suitable protocol for primary protection. The GOOSE object within IEC 61850 is designed for high-speed protection and control applications. IEC 61850 GOOSE automatically broadcasts messages containing status, controls, and measured values onto the network for use by other devices. GOOSE sends the message several times, increasing the likelihood that other devices receive the messages.

The object-oriented peer-to-peer data exchange capabilities are the most significant properties of IEC 61850 over the other common standards. The Substation configuration language (SCL) is an XML-based configuration language used to support the exchange of configuration data between different tools from different vendors. There are four types of SCL files as follows.

- IED capability description file (ICD).
- System specification description (SSD) file.
- Substation configuration description file (SCD).
- Configured IED description file (CID).

The ICD file describes the capabilities of an IED, including information on LNs and GOOSE. The SSD file describes the single-line diagram of the substation and the required LNs. The SCD file contains all IEDs, communications configuration data, and a substation description. The CID file describes a single instantiated IED within the project and includes address information. For ease of usage, every vendor will provide an editor with a user interface to parse the SCL files. In this case, RTDS has ICT editor [25] and SEL has AcSELerator Architect.

The data model in IEC 61850 follows a hierarchical structure with each physical IED consisting of several logical devices representing physical equipment. Each logical device has several logical nodes (LN). Logical nodes (which are abstract) are the IEC 61850 object-oriented virtual model's primary elements, consisting of standardized Data Objects (DO) and Data Attributes (DA) [24]. Most data objects comprise standard classes involving basic data objects, status, control, and measurement. Each data element consists of several data attributes with a data attribute type that belongs to functional constraints. The proposed protection scheme uses the Generic process I/O (GGIO) LN defined to use for non-standard functions. The calculated direction measurements and breaker status in the IED model described in section III-A2 are mapped to status information DO-Ind and DA-"stVal". The Analog Input DO-AnIn is used for voltage measurements from the IED model and values are mapped to DA-"mag.f". The trip signals from the relay described in section III-C are also defined as GGIO LN and mapped to DO-Ind, DA-"stVal".

With the decided data models, the steps to complete the configuration of GOOSE messaging between RTDS and SEL-421 relay is as follows.

1) Using the ICT editor in RSCAD, map the outputs of IEDs (current directions, breaker status, RMS voltages) described in section III-A2 to correct data models and configure them to publish as GOOSE messages.
2) Export the configured settings as a CID file from ICT editor and import it on SEL Architect.
3) In SEL Architect, Map the DAs to the virtual bits and analog inputs according to section III-C in the relay. This step will ensure relay subscribing to messages from RTDS.
4) Create GOOSE transmit messages using protection variables (PSVXX) for publishing trip messages.
5) Export the CID file for the SEL relay and import it in ICT editor and configure to subscribe to the trip messages from SEL relay.

The data flow between RTDS and SEL 421 relay for the configured IEC61850 communication is show in Fig. 4.

E. Microgrid controller and TCP/IP link

The TCP/IP is a standard communication protocol that establishes end-to-end communication with acknowledgments ensuring packet delivery. The TCP standard comes with priority settings that can be used to prioritize the protection related

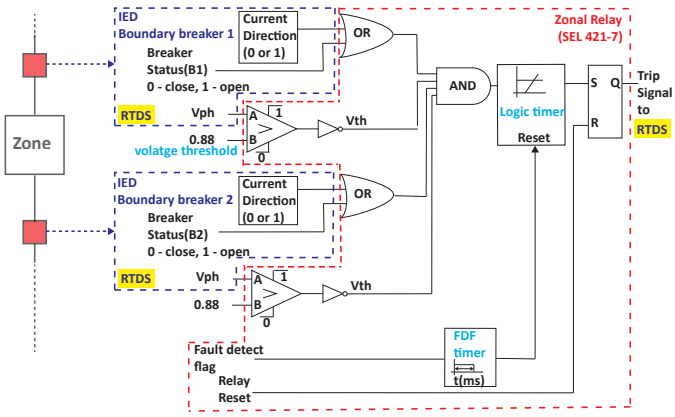

Fig. 5. Primary protection fault detection logic with two boundary breakers.

data over the network to warrant faster packet delivery. To protect the entire microgrid, the physical network design covering the whole area to yield the 4ms end-to-end latency requirement of IEC61850 can be achievable [26] but can increase the cost of implementation. For the backup protection an extra time delay is available to operate as it is time co-coordinated with primary protection (100ms in this paper). Hence, TCP/IP with a latency of around 10ms to 20ms [27] can be a suitable protocol for backup protection. The backup protection and reconfiguration logic are programmed in MATLAB on the runtime computer shown in Fig. 2. The *tcpclient* object in MATLAB software can be used to represent a connection to a remote host and remote port from MATLAB to read and write data. The remote host can be a server or hardware that supports TCP/IP communication. In this case, RTDS is configured as a TCP server supporting bi-directional data. The server is configured with an IP address and port number to send/receive data. The data flow between RTDS and MATLAB program in microgrid controller (i.e., runtime PC) for the configured TCP/IP is shown in Fig. 4. The current directions, voltage values, breaker status and trip signals from primary protection are formatted into a data array and sent as IP packets. The IP packets are read at the runtime computer and the payload is extracted and sent to back up protection and reconfiguration programs. After program execution, the trip signals from backup protection are sent back to the server (RTDS) from MATLAB as IP packets. Similarly, close signals from the reconfiguration program are sent to RTDS from MATLAB.

IV. Implementation of the Protection Scheme

The IEC 60834-1: Teleprotection Equipment of Power Systems defines the fault clearance times for communication assisted protection schemes. The time divisions of the total fault clearing time includes several parts as shown in Table I. If protection applications requires transmitting and receiving information from a remote location, propagation delays for teleprotection needs to be taken into account as well. In summary, the typical fault clearance time can be in the range of 42ms to 180ms. However, the fault clearance time has to be selected to achieve fast isolation of fault adhering to selectivity, sensitivity, reliability and co-ordination with any downstream protection devices/schemes.

TABLE I
Time Allocation for Fault Clearance According to IEC60834-1

Category	***details***	***time (ms)***
Fault recognition time	-Analog to digital conversion -protection algorithm pickup	10 to 30
Teleprotection	-network latency and propagation delay for teleprotection	2 to 40
Relay decision time	-Trip decision in application -relay operating time	0 to 30
circuit breaker operating time	-circuit breaker trip coil -circuit breaker mechanical movement	30 to 80
Total	Fault clearance time for a protection system	42 to 180

As discussed in section II, The protection scheme includes primary and back-up protection. Three settings are required for the primary protection logic of a zone shown in Fig. 5: 1) logic timer, 2) voltage threshold, and 3) Fault Detect Flag (FDF) timer, where the settings used are 2 cycles (33ms), 0.88 PU, and 100ms respectively. The detailed explanantion of the logic and flags are given in [12]. Based on the primary protection logic timer, backup protection time delay has to be set by adding the co-ordination time interval (CTI) to logic timer. Unlike conventional protection schemes where CTI includes relay and breaker operation time, the CTI in this scheme should include maximum network latency and operation delays as it involves communication.

The detailed time division of total fault clearance by primary protection is shown with an example: a BG fault is applied in zone 1, that has three boundary breakers B1, B2 and B9. The communication setup for the example is shown in Fig. 6 (a). The time taken for different operations in ms is shown in Fig. 6 (b). The fault is applied at 20ms, where as the relay picked up the fault at 39ms after the voltage went below threshold of 0.88PU. The relay decision time and round trip communication took around 43ms (33ms of time delay + 8ms for round trip communication and relay logic execution) to receive trip signal at the breakers B1, B2 and B9 at 82ms. The breaker opening delay is 35ms, taken from the data sheet of the breaker equipment assumed in the paper [23]. So, the total fault clearing time is around 97ms, which is within the IEC 60834 specified range.

Now, considering to have a network that can provide a maximum communication latency of 4ms for for IEC61850 communication and 10ms for TCP/IP, The CTI should be at least: 33ms (logic timer) + (2*4ms) + 10ms = 51ms. The backup time delay has to be set $>$ 35ms (breaker opening time) + CTI = 86ms. In this paper, the time delay of 100ms is selected for the backup protection allowing enough time for co-ordination with primary protection. For the same BG fault in zone 1, the time of operation in ms for backup protection is shown in Fig. 6 (c). The fault is applied at 20ms and backup protection picked up the fault at 39ms after the voltage went below threshold of 0.88PU. The program decision time and round trip communication took around 120ms to receive trip signal at the breaker at 160ms. The 120ms include 100ms time delay, 12ms for execution of backup protection program

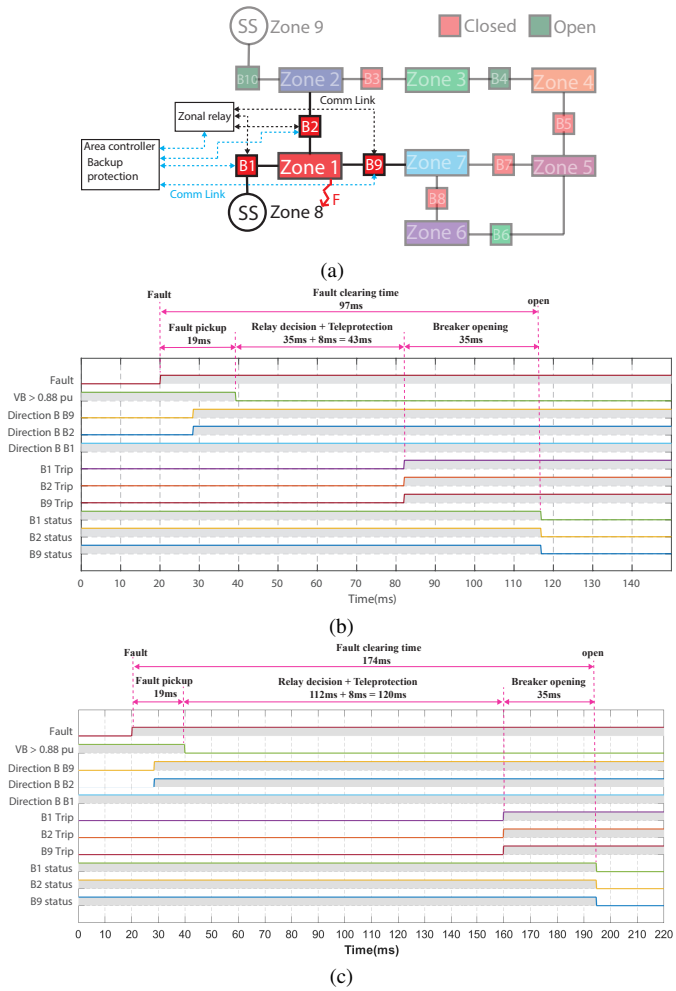

Fig. 6. Protection of zone 1: (a) communication setup, (b) operating times of primary protection, (c) operating times of secondary protection.

execution and 8 ms for round trip communication. Considering the breaker opening time, the total fault clearing times is around 174ms, which is within the IEC 60834 range.

V. Results

The Protection scheme was tested on the 123 node distribution feeder using the HIL setup discussed in section III. The Following case studies in this section are used for the analysis and validation of the proposed scheme on the co-simulation platform.

A. Primary Protection

The primary protection logic for all seven zones is programmed in the SEL-421 relay. The protection scheme is tested in real-time for different faults in different parts of the 123-bus feeder in both grid-connected and islanded modes. The response of the scheme in detecting, locating, and clearing the faulted zone at three randomly selected locations on the feeder in grid-connected mode is shown in Fig. 7 (a) and islanded mode is shown in Fig. 7 (b). It can be seen that in both modes of operation, correct zonal protection is detecting the fault and sending the trip signal. For example, in Fig. 7

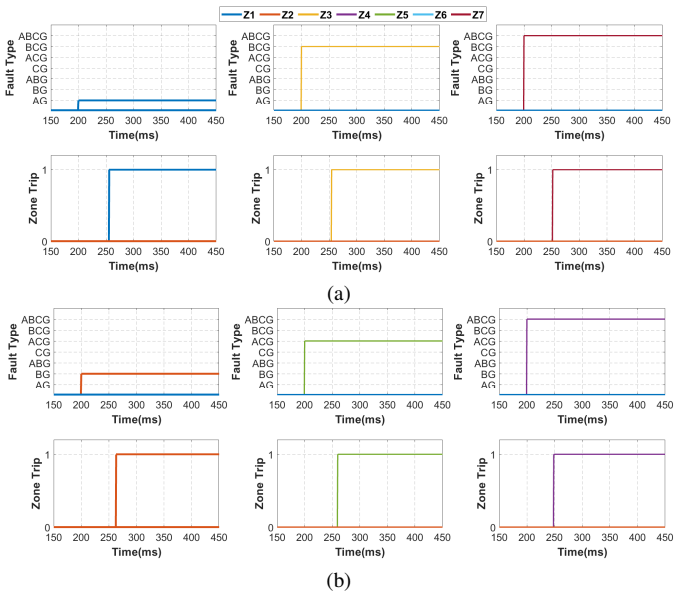

Fig. 7. Primary protection response: (a) grid connected mode, (b) islanded mode

(a), an AG fault at 200 ms in zone 1 is detected by the zone 1 relay (blue color), and the zone trip signal is received by corresponding breakers B1, B2 and B9 at 255 ms in RTDS run time. The operation time of 55 ms includes the pick up time, relay operation and round trip time communication delay. The actual breaker opens 35ms after receiving trip signal.

B. Backup Protection

The backup protection is tested for three cases: primary protection failure, breaker failure, and IED communication failure in both grid-connected and islanded modes of operation. As mentioned in the previous section IV, to co-ordinate with the primary protection, a time delay of 6 cycles (100ms) is used in the backup protection logic. First, for a primary protection failure, the response of the backup protection for detecting, locating, and clearing the faulted zone at three randomly selected locations on the feeder in grid-connected mode is shown in Fig. 8. For example, for an ACG fault in zone 1 at 200ms, the backup protection will trip the breakers B1, B2, B9 at 330ms and isolate zone 1. The operation time of 130 ms includes the 100 ms of time delay plus 30 ms for relay pickup time, backup protection operation and communication delay. Second, for a breaker failure, the response of the backup protection is demonstrated with a test case in islanded mode, as shown in Fig. 9(a) and (c). For a BG fault at 200ms in zone 4, when breaker B5 fails to operate (the breaker failure signal is simulated at 285 ms), the backup protection will clear the faulted region (zone 4 and 5) by opening breakers B6, B7 at 348ms. The operation time of 148 ms includes the 100 ms of time delay plus 48 ms for round trip relay pickup time, backup protection operation (decide the next breakers to trip for the failed breaker) and communication delay. Third, for an IED communication failure, the response of the backup protection is demonstrated with a test case in islanded mode, as shown in Fig. 9(b) and (d). For an ABCG fault at 200ms in zone 4,

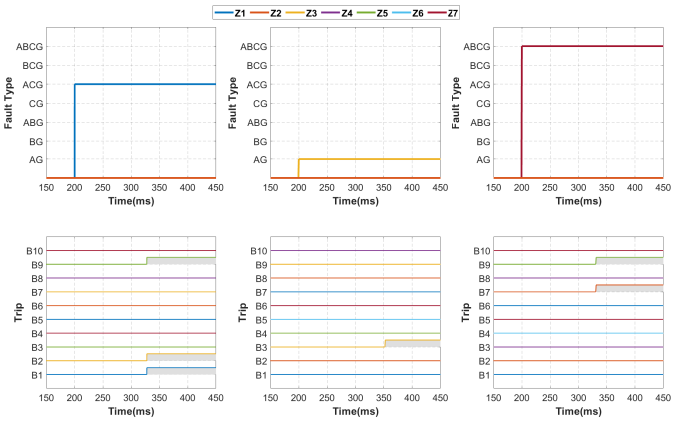

Fig. 8. Backup protection response to primary protection failure

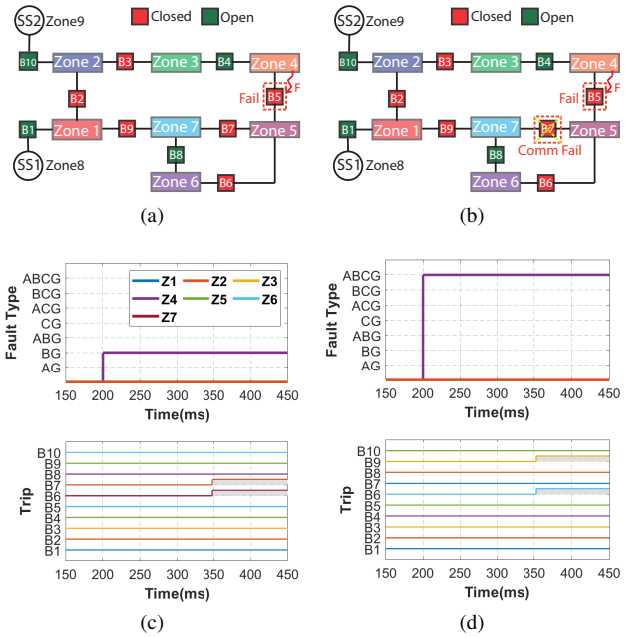

Fig. 9. Backup protection response to: (a) breaker failure, (b) IED failure (c) fault type and breaker trip signals for breaker failure, (d) fault type and breaker trip signals for IED failure

when breaker B5 fails to operate (the breaker failure signal is simulated at 285 ms) in addition to IED comm failure at B7, the backup protection will clear the faulted region (zone 4, 5, and 7) by opening breakers B6, B9 at 352ms. The operation time of 152 ms includes the 100 ms of time delay plus 52 ms for round trip communication delay, relay pickup time plus backup protection logic operating time in expanding the protection region for the failed IED and deciding the next breaker(s) to trip for the failed breaker. Note that the trip time shown in the figures is the time when the breaker will receive a trip signal.

C. Reconfiguration aided Protection

The first case is to demonstrate the working of the reconfiguration program in self healing the system in the event of loss of grid source. A temporary fault is applied in zone 1 on the base case topology shown in Fig. 1 (b) and the zonal relay will isolate the fault by tripping breakers B1, B2, and B9. This action by the protection system leads to the loss of grid source SS1 to the healthy part of the system (i.e. zone 2, 3, 4, 5, 6, and 7). In this case, the reconfiguration program connects the healthy part of the system to an alternative grid source (SS2) by closing breakers B10 and B3. The topology after reconfiguration is shown in Fig. 10(a). The power plots in Fig. 10 (c) show stable reconfiguration for this case. As the fault is temporary, zone 1 will be reconnected to the system by the reconfiguration program (after clearing the fault flag manually) by closing breaker B2. The next case is executed on this changed topology in Fig. 10(a).

The second case will exhibit the robustness of the reconfiguration program to work for any topology. A permanent fault is applied in zone 4, and the protection system isolates the fault by opening breakers B4 and B5. This action will lead to the islanding of healthy zones (i.e. zone 5, 6, and 7). The reconfiguration program closes breaker B9 to connect the healthy zones to the grid source. The topology after reconfiguration is shown in Fig. 10 (b). The power plots shown in Fig. 10 (d) show stable reconfiguration for this case. As the fault is permanent, it can be seen that the IBR 7 and 8 will shut down after they ride through the fault (see the power output goes to zero) in accordance with the requirements of IEEE1547 standard.

D. Reconfiguration for a fault with equipment failure

The case will demonstrate the isolation of the faulted zone by backup protection for a breaker failure followed by reconfiguration program self-healing the rest of the healthy system. For a temporary fault in zone 7 on the base case topology shown in Fig. 1 (b), the breakers B9 and B7 are tripped by zone 7 relay at 252ms. when breaker B9 fails to operate, the backup protection will clear the faulted region (zone 1 and 7) by opening breakers B1, B2 at 345ms as shown in Fig. (a), (c). The reconfiguration program detects two healthy islands (zone 2, 3 and zone 4, 5 ,6) and loss of grid source SS1. It connects the healthy island zones 2, 3 to next available grid source SS2 by closing breaker B10 at 1.6s and the other island of healthy zones 4, 5, and 6 by closing breaker B4 at 3.8s. The topology after reconfiguration is shown in Fig 11(b). The power plots for these events of fault isolation and stable reconfiguration are shown in Figure 11 (d).

VI. Conclusion

This paper implemented a HIL platform capable of modeling the data flow between the RTDS and physical protective devices to protect a utility-scale microgrid. The co-simulation framework utilizes a real communication network built using IEC61850 for the primary protection and TCP/IP protocol for the backup protection and reconfiguration. The significance of this framework is that it can not only integrate commercially available protective relays, but also protection and control logic programmed on a generic computer to validate the protection methods in real time. The protection scheme is tested on the highly unbalanced IEEE 123-node feeder with

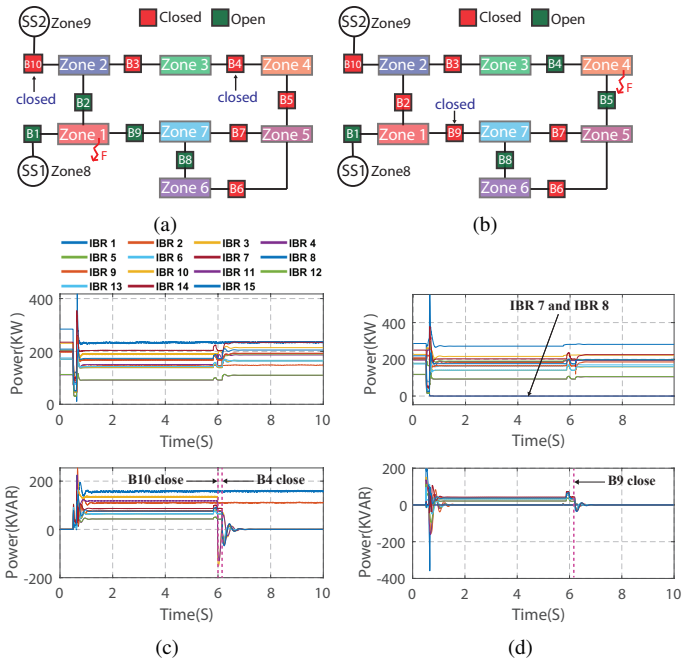

Fig. 10. (a) Topology post reconfiguration case 1, (b) topology post reconfiguration case 2, (c) IBRs power output for case 1, (d) IBRs power output for case 2

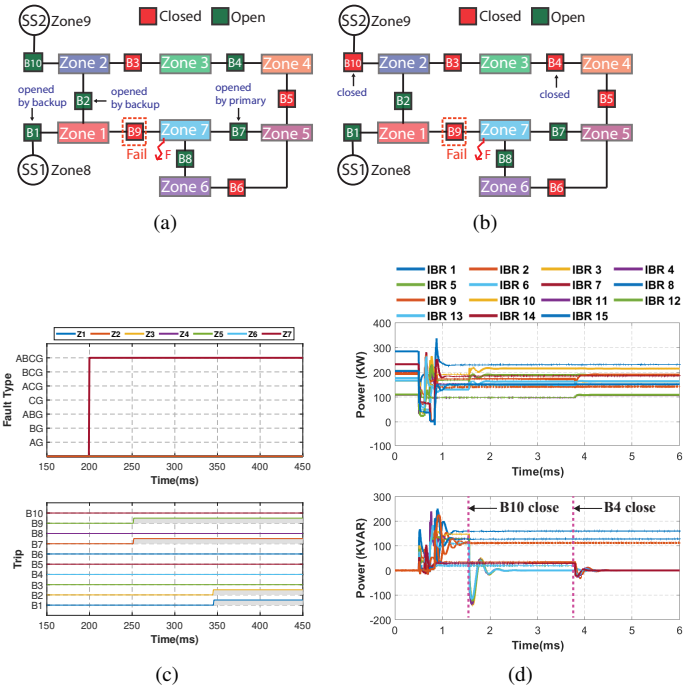

Fig. 11. (a) Topology after fault isolation, (b) Topology after reconfiguration, (c) protection system response, (d) IBRs power output

15 IBRs connected to it. Reliable operation of main and backup protection is demonstrated without the need for any adaptive changes in settings for grid-connected or islanded modes. The Backup protection comprehensively addresses failure of primary protection relay, breaker or communication. The Reconfiguration scheme is tested to show temporary faults do not result in permanent outage and dynamic self healing of the healthy part of the system. The successful testing of holistic protection and reconfiguration scheme on IEEE 123 node feeder in real-time demonstrates the smooth flow of data between the cyber and physical parts in the system to protect and self-heal the microgrid under test.

REFERENCES

[1] A. Hooshyar and R. Iravani, "Microgrid protection," *Proceedings of the IEEE*, vol. 105, no. 7, pp. 1332–1353, 2017.

[2] S. Brahma, "Protection of distribution system islands fed by inverter-interfaced sources," in *2019 IEEE Milan PowerTech*, 2019, pp. 1–6.

[3] H. Al-Nasseri and M. A. Redfern, "Harmonics content based protection scheme for micro-grids dominated by solid state converters," in *2008 12th International Middle-East Power System Conference*, 2008, pp. 50–56.

[4] J. Duan, K. Zhang, and L. Cheng, "A novel method of fault location for single-phase microgrids," *IEEE Transactions on Smart Grid*, vol. 7, no. 2, pp. 915–925, 2016.

[5] X. Li, A. Dyśko, and G. M. Burt, "Traveling wave-based protection scheme for inverter-dominated microgrid using mathematical morphology," *IEEE Transactions on Smart Grid*, vol. 5, no. 5, pp. 2211–2218, 2014.

[6] T. Patel, S. Brahma, J. Hernandez-Alvidrez, and M. J. Reno, "Adaptive protection scheme for a real-world microgrid with 100resources," in *2020 IEEE Kansas Power and Energy Conference (KPEC)*, 2020, pp. 1–6.

[7] S. B. A. Bukhari, C. Kim, K. K. Mehmood, R. Haider, and M. Saeed Uz Zaman, "Convolutional neural network-based intelligent protection strategy for microgrids," *IET Generation, Transmission Distribution*, vol. 14, no. 7, pp. 1177–1185, 2020.

[8] N. Fawzy, H. F. Habib, O. Mohammed, and S. Brahma, "Protection of microgrids with distributed generation based on multiagent system," in *2020 IEEE International Conference on Environment and Electrical Engineering and 2020 IEEE Industrial and Commercial Power Systems Europe (EEEIC / I CPS Europe)*, 2020, pp. 1–5.

[9] C. Yuan, K. Lai, M. S. Illindala, M. A. Haj-ahmed, and A. S. Khalsa, "Multilayered protection strategy for developing community microgrids in village distribution systems," *IEEE Transactions on Power Delivery*, vol. 32, no. 1, pp. 495–503, 2017.

[10] S. Mirsaeidi, D. M. Said, M. W. Mustafa, M. H. Habibuddin, and K. Ghaffari, "Progress and problems in micro-grid protection schemes," *Renewable and Sustainable Energy Reviews*, vol. 37, pp. 834–839, 2014.

[11] K. Hansen, C. Breyer, and H. Lund, "Status and perspectives on 100% renewable energy systems," *Energy*, vol. 175, no. 11, pp. 471–480, May 2019.

[12] P. H. Gadde and S. M. Brahma, "Topology-agnostic, scalable, self-healing and cost-aware protection of microgrids," *IEEE Transactions on Power Delivery*, pp. 1–1, 2021.

[13] P. H. Gadde, S. Brahma, and T. Patel, "Scalable protection and self-healing of microgrids: Hardware in the loop co-simulation," in *2022 IEEE Texas Power and Energy Conference (TPEC)*, 2022, pp. 1–6.

[14] K. sidwall and P. Forsyth, "Advancements in real-time simulation for the validation of grid modernization technologies," *Energies*, vol. 13, no. 16, p. 4036, 2020.

[15] H. F. Habib, N. Fawzy, and S. Brahma, "Performance testing and assessment of protection scheme using real-time hardware-in-the-loop and iec 61850 standard," *IEEE Transactions on Industry Applications*, vol. 57, no. 5, pp. 4569–4578, 2021.

[16] *RTDS Hardware Manual*, RTDS Technologies, 03 2020.

[17] P. H. Gadde and S. Brahma, "Comparison of pr and pi controllers for inverter control in an unbalanced microgrid," in *2020 52nd North American Power Symposium (NAPS)*, 2021, pp. 1–6.

[18] T. Patel, P. H. Gadde, S. Brahma, J. Hernandez-Alvidrez, and M. Reno, "Real-time microgrid test bed for protection and resiliency studies," in *2020 North American Power Symposium (NAPS)*, 2020, pp. 1–6.

[19] J. Svensson, M. Bongiorno, and A. Sannino, "Practical implementation of delayed signal cancellation method for phase-sequence separation," *IEEE Transactions on Power Delivery*, vol. 22, no. 1, pp. 18–26, Jan 2007.
[20] M. J. Reno, S. Brahma, A. Bidram, and M. E. Ropp, "Influence of inverter-based resources on microgrid protection: Part 1: Microgrids in radial distribution systems," *IEEE Power and Energy Magazine*, vol. 19, no. 3, pp. 36–46, 2021.
[21] J. L. Blackburn and T. J. Domin, *Protective Relaying, Principles and Applications*, 3rd ed. New York: CRC Press, 2006, ch. 3, pp. 94–101.
[22] D. L. Ransom, "Get in step with synchronization," in *2014 67th Annual Conference for Protective Relay Engineers*, 2014, pp. 401–407.
[23] Siemens AG, "Siemens Vacuum Recloser 3AD." [Online]. Available: https://assets.new.siemens.com/siemens/assets/api/uuid:2573ed46-a618-45e5-bcdf-40b8f511dd5f/hg-11-42-en.pdf
[24] F. Clavel, E. Savary, P. Angays, and A. Vieux-Melchior, "Integration of a new standard: A network simulator of iec 61850 architectures for electrical substations," *IEEE Industry Applications Magazine*, vol. 21, no. 1, pp. 41–48, 2015.
[25] *RSCAD IEC61850 IED configuration tool*, RTDS Technologies, 03 2020.
[26] J. M. Herrera, M. S. Mingarro, S. L. Barba, D. Dolezilek, F. Calero, A. Kalra, and B. Waldron, "Case study of time-domain automation and communications: Field-proven benefits to automation, control, monitoring, and special protection schemes," in *2017 Saudi Arabia Smart Grid (SASG)*, 2017, pp. 1–8.
[27] G. Ravikumar, D. Ameme, S. Misra, S. Brahma, and R. Tourani, "An information-centric network architecture for wide area measurement systems," *IEEE Transactions on Smart Grid*, vol. 11, no. 4, pp. 3418–3427, 2020.

Phani Gadde (S'2015) received B.Tech. degree from Jawaharlal Nehru Technological University, India, in 2013 and M.S. degree in Electrical Engineering from New Mexico State University, USA, in 2015. He worked as Power Systems Engineer at ABB Enterprise software Inc from 2016 to 2018. He is currently a PhD student at Clemson University.

Sukumar M. Brahma (F'2020) is Dominion Energy Distinguished Professor of Power Engineering and Director of Clemson Electric Power Research Association (CUEPRA) at Clemson University. He has been past editor and Guest EIC for IEEE Transactions on Power Delivery.

Trupal Patel (S'2015)Trupal Patel received a M.Sc in electrical engineering degree from Clemson university, south carolina, USA in 2020, where he is currently pursuing the Ph.D. degree in electrical engineering. His current research interests include power system stability and protection with high penetration of distributed energy resources